

# Improving Interfacial Adhesion of PLA/Lignin Composites by One-Step Solvent-Free Modification Method

Ningning Wang<sup>1</sup>, Caili Zhang<sup>1,2,\*</sup>, Wenqin Zhu<sup>3</sup> and Yunxuan Weng<sup>1,2,\*</sup>

<sup>1</sup>School of Materials and Mechanical Engineering, Beijing Technology and Business University, Beijing, 100048, China

<sup>2</sup>Beijing Key Laboratory of Quality Evaluation Technology for Hygiene and Safety of Plastics, Beijing Technology and Business University, Beijing, 100048, China

<sup>3</sup>Petrochemical Research Institute, PetroChina, Beijing, 102206, China

\*Corresponding Authors: Caili Zhang. Email: zhangcaili@btbu.edu.cn; Yunxuan Weng. Email: wyxuan@th.btbu.edu.cn

Received: 30 January 2020; Accepted: 13 May 2020

**Abstract:** To clarify the effects of lignin as a biodegradable filler added into the PLA matrix, PLA/lignin composites with or without silane coupling agent of  $\gamma$ -(2,3-epoxypropoxy)propyl trimethoxysilane (KH560) were prepared by a one-step solvent-free modification method. The effects of KH560 as a compatibilizer on the morphology, chemical structure, crystallization behavior, thermal degradative behavior as well as mechanical strength of the PLA/lignin composites were analyzed in detail. It was found that, after modification by KH560, the fractured surfaces of composites became smooth, suggested sufficient bonding between the lignin and PLA in the composites with KH560 coupling agent molecules. This result further proved by <sup>1</sup>H NMR and ATR spectra of the composites that lignin and PLA formed stable chemical bonds with KH560. Due to the toughening effect of KH560, mainly affect the molecular chain mobility, the thermodynamic properties of LG-KH560/PLA composites were all reduced. When compared to the conventional solution modification method of adding silane coupling agents into PLA/lignin, the composites were synthesized via a single-step reactive extrusion modification procedure in this work showed relatively low tensile strength, which mainly because the existence of the free radicals due to coupling agents result in the composite's deterioration and subsequent weakening of the tensile properties.

**Keywords:** PLA; lignin; composites; interfacial adhesion; reactive extrusion

## 1 Introduction

One of the prominent biodegradable polyesters available commercially is Poly (lactic acid) (PLA), which is a bioplastic. However, PLA suffers from issues such as being intrinsically brittle, degrades slowly, and is relatively expensive. PLA is not yet regarded as a candidate to be straight substitute for traditional petroleum-based polymers. One compelling method to overcome this constraint is to incorporate other materials as a filler to produce a composite. Over the last decade, large efforts have been directed to prepare PLA-based composites with different biodegradable or non-biodegradable filler materials to enhance or increase its performance [1–5].



This work is licensed under a Creative Commons Attribution 4.0 International License, which permits unrestricted use, distribution, and reproduction in any medium, provided the original work is properly cited.

As the next most plentiful natural biopolymer after cellulose, lignin is renewable resource and mainly comes from by-product of and bio-refinery and paper industries [6]. It is a disordered polymer with diverse structures, which contains interlinked units of guaiacyl, syringyl and p-hydroxyphenyl, moieties [7,8]. As it possesses numerous carbonyl, carboxyl, hydroxyl and methyl groups on its surface, lignin is a good candidate for making bio-based polymeric composites to alter material properties such as hydrophobicity, stiffness, and crystallinity [9,10]. Therefore, the combination of PLA and lignin is a promising combination for an environmentally-friendly and cutting-edge material [11,12].

The interface bonding and size of particle matter strongly to how the lignin strengthens the polymer matrix. [13]. On the other hand, the interface is crucial to the mechanical properties, e.g., load transfer and bond distribution [14]. The non-compatibility of chemical and physical properties of the matrix and lignin results in poor bonding at the interface, weak dispersion and overall low quality of the composite. [15]. Therefore, the most important aspect for the formulation of lignin composites with exceptional physical properties is improving the effectiveness of the interfacial adhesion between the reinforcing lignin and polymer matrix. Different ways of modifying the composites with the intention of solving with non-compatibility and fine-tuning of the interfacial adhesion between polymer and lignin were reported and the most effective way to overcome this was through chemical modifications [16,17].

As lignin contains numerous hydroxyl groups, with the correct chemicals it can result in new reactive sites forming, such as epoxy, amine and carboxylic on its surface. The silane coupling agent of  $\gamma$ -(2,3-epoxypropoxy) propyl trimethoxysilane (KH560) is a widely used compatibilizer for it contains highly reactive epoxy groups, which could easily react with carboxyl terminal group of PLA [18,19]. The introduction of KH560 into the PLA/lignin composites can be through solution treatment or via reactive extrusion two different methods.

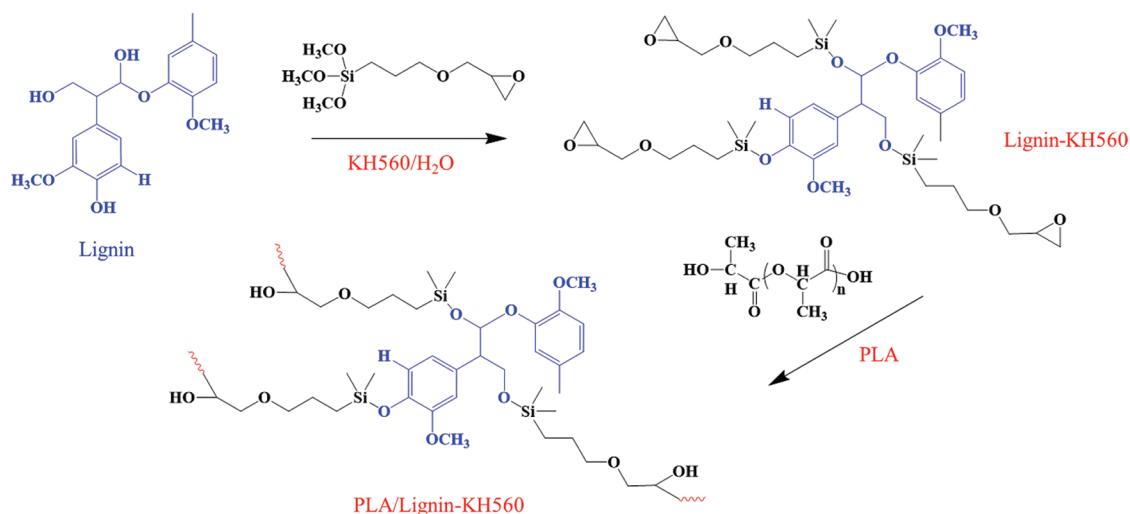
Zhu et al. [20] has used KH560 to modify PLA/lignin composites by solution treatment method. First, silane coupling agent was dissolved in water/ethanol solution to make the 2 wt.% KH560 solution, and then the lignin powder was treated by the prepared solution at 105°C for 12 h. As a result, when compared to the PLA/lignin composite without coupling agent, the tensile strength of the prepared 20 wt.% lignin content PLA-based composite showed significant increase from 43 to 53 MPa, due to the enhanced interfacial adhesion. By comparison with solution treatment method, reactive extrusion (in situ melt blending in an extruder) is solventless, green and can be mass-produced with little effort.

In this work, the effects of KH560 as a compatibilizer to enhance the mechanical strength of PLA-lignin composites by reaction extrusion method were investigated. A one-step process of integrating PLA and lignin straight and subsequent incorporating KH560 in the Haake Rheometer to make LG-KH560/PLA composites was used; the reaction mechanism was showed in Scheme 1. In details, morphology, chemical structure, crystallization behavior, thermal degradative behavior as well as mechanical strength of the PLA/lignin composites with or without KH560 compatibilizer have been fully evaluated as a function of renewable composition.

## 2 Experimental

### 2.1 Materials

PLA was supplied by Natureworks (4032D,  $M_n = 88500$  g/mol,  $M_w/M_n = 1.8$ ). Lignin (CAS No. 9005-53-2) was procured from J & K Scientific Ltd., as the powder form ( $\geq 200$  mesh), which is soluble in chloroform. The molecular weight of lignin is 2265 g/mol. The silane coupling agent of  $\gamma$ -(2,3-epoxypropoxy) propyl trimethoxysilane (KH560) was purchased from Tianjin Fu Chen Chemical Reagents Factory (China) and use as-is with no purifying.



**Scheme 1:** The reaction mechanism between coupling agent KH560 with PLA and lignin

## 2.2 Composites Fabrication

PLA-lignin composites in this work with various make-ups were synthesized with raw materials mentioned above. [Tab. 1](#) lists the code name based on the composition. PLA and lignin were desiccated at 60°C with a vacuum oven for 48 h to eliminate moisture before use. The silane coupling agent was prepared to 90% solution in water. All the composite samples were made using a Haake Rheometer at 190°C and 70 rpm for about 6 min. PLA and lignin with different weight ratios were mixed beforehand in the chamber until the torque stabilizes became stable (ca. ~2 min), then the dynamic vulcanization was completed until the melt torque leveled off. Subsequently, the melting mixed samples were taken out from the internal mixer's cavity and cooled down to room temperature. To evaluate the effect of KH560 on the performance of PLA/lignin composites, the prepared solution containing the silane coupling agent was injected into the mixer after lignin was added. The extruded composite samples were pelletized and then injection molded using a miniature version of injection molding machine (Haake MiniJet, Thermo Fisher Scientific). The temperature of the mini-injection molding system was set at 180°C and the mold remained at room temperature. Dumbbell-shaped specimens (ISO 37, type 2) and cuboid-shaped specimens (40 mm × 10 mm × 1 mm) were custom-made for testing.

**Table 1:** Composition of PLA and its composites

Designation	PLA (wt%)	Lignin (wt%)	KH560 (phr)
PLA	100	0	0
1%LG/PLA	99	1	0
3%LG/PLA	97	3	0
5%LG/PLA	95	5	0
1%LG-KH560/PLA	99	1	2
3%LG-KH560/PLA	97	3	2
5%LG-KH560/PLA	95	5	2

### 2.3 Characterizations

Using scanning electron microscopy (SEM; Quanta 250 FEG, FEI), the composites' morphology was characterized. The attenuated total reflection mode FTIR (ATR-FTIR) spectra of the samples were determined using a PerkinElmer 782 Fourier transform spectrophotometer. In transmission mode set to a resolution of  $4\text{ cm}^{-1}$ , 32 scans were collected in total, spanning across  $4000\text{ to }600\text{ cm}^{-1}$ . Nuclear magnetic resonance ( $^1\text{H NMR}$ ) spectra were taken down with a Bruker AVANCE III HD 400 MHz spectrometer in  $\text{CDCl}_3$ . As for Thermogravimetric analysis (TGA), it was conducted with a Hitachi instruments STA7200 in a  $\text{N}_2$  atmosphere at a heating rate of  $10\text{ }^\circ\text{C}/\text{min}$ . Differential scanning calorimetry (DSC) was performed on a Hitachi Instruments DSC7020 at a heating rate of  $10\text{ }^\circ\text{C}/\text{min}$  from  $30\text{--}200\text{ }^\circ\text{C}$  under  $\text{N}_2$  whose flow was  $200\text{ ml}/\text{min}$ . The samples were measured with 2 successive scans. The thermal history of the samples were erases with the first heating and cooling cycle. For every sample, the glass transition temperature ( $T_g$ ) of each sample was measured based on the second heating curve's mid-point transition temperature. The  $T_g$  of each sample were also analyzed by a Hitachi Instruments DMA7100 equipment used cuboid-shaped specimens ( $40\text{ mm} \times 10\text{ mm} \times 1\text{ mm}$ ) made by injection molding. Samples were tested in a tension mode with temperature spanning across  $30\text{ }^\circ\text{C}$  to  $110\text{ }^\circ\text{C}$  with a heating rate of  $3\text{ }^\circ\text{C}/\text{min}$ , with a loading amplitude of  $10\text{ }\mu\text{m}$ , a dynamic force of  $1\text{ N}$  at  $10\text{ Hz}$ . Tensile tests were performed at room temperature according to ASTM D638 using a universal test machine. Pitch was settled at  $50 \pm 0.25\text{ mm}$ . Strain rate was  $3\text{ mm}/\text{min}$ . Load cell was  $500\text{ N}$ . Spindles were dumbbell shape (Length:  $\geq 150\text{ mm}$ , Width:  $10 \pm 0.2\text{ mm}$ , Thickness:  $4.0 \pm 0.2\text{ mm}$ ). A minimum of 5 specimens were studied per sample and mean data were tabulated.

## 3 Results and Discussion

### 3.1 The Morphology of LG/PLA and LG-KH560/PLA Composites

The dispersion and compatibility of lignin in the PLA with and without compatibilizer KH560 was analyzed by SEM images. The micrographs of the composite's fractured surfaces were shown in Fig. 1. For 3%LG/PLA and 5%LG/PLA, it can be observed that both composites without compatibilizer (Figs. 1c and 1e) exhibited agglomeration due to the poor compatibility between lignin and PLA, these composites displayed spheroidal-like lignin particles incorporated inside the matrix (highlighted by the red circles on the micrographs). After modification by KH560, the fractured surfaces of composites became smooth. This observation suggested sufficient bonding at the interface between the lignin and

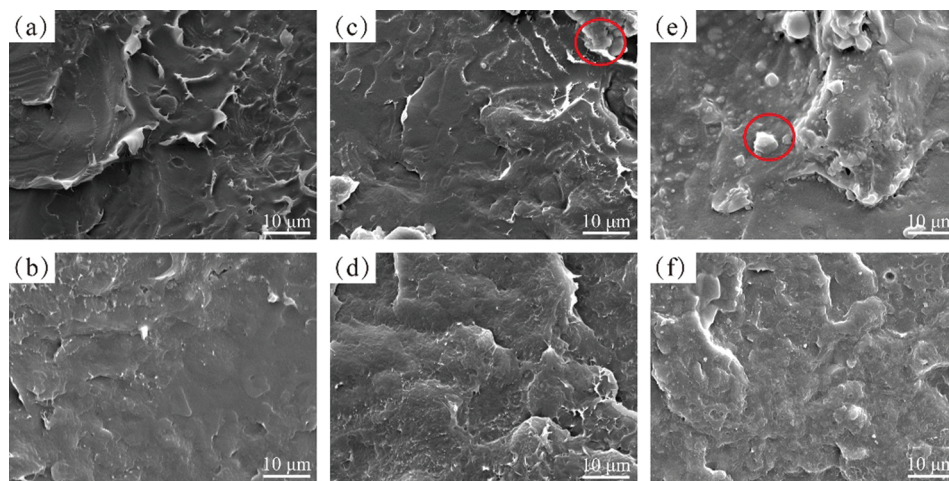


**Figure 1:** SEM micrographs depicting the fractured surfaces of composites (a) 1%LG/PLA, (b) 1%LG-KH560/PLA, (c) 3%LG/PLA, (d) 3%LG-KH560/PLA, (e) 5%LG/PLA, (f) 5%LG-KH560/PLA

PLA in the composites with KH560 coupling agent molecules, demonstrating that between the hydroxyl groups on the lignin surface and carboxylic acid terminal groups of PLA formed stable chemical bonds with KH560. This reaction was further confirmed by  $^1\text{H}$  NMR and ATR spectra of the composites.

### 3.2 The Structure of LG/PLA and LG-KH560/PLA Composites

Fig. 2 shows the ATR spectra of pure PLA and its composites. For the pure PLA, the strong spectra band at about  $1745\text{ cm}^{-1}$  was ascribed to C=O stretching vibration of the ester groups. After addition lignin (amount varying from 1 wt% to 5 wt%), these absorption peaks were almost the same as that of pure PLA. This could be ascribed to the weak interaction between the lignin and the matrix. While after addition of KH560, at around  $1753\text{ cm}^{-1}$ , a sharp and strong peak was observed due to stretching vibration of carbonyl groups, correspond to the new ester group formed between carboxylic acid of group of PLA and epoxy group of KH560. Also, around  $2852\text{ cm}^{-1}$  appeared C–H stretching vibration in  $-\text{CH}_2$  groups of KH560. This indicated that the chemical reaction occurred between PLA and KH560. Because of the relatively low content, the characteristic peak of lignin is not obvious. The reaction occurred between lignin and KH560 was confirmed by  $^1\text{H}$  NMR analysis, as shown in Fig. 3. For unadulterated PLA, the characteristic single peaks at 1.57–1.59 ppm, and 5.20 ppm were due to methyl protons and methylene protons in PLA side chains, respectively. After addition of 1 wt% lignin in the matrix, the signal at 1.53 ppm was related to the aliphatic moiety in the lignin. When the composite was modified by KH560, a signal at 3.57 ppm appeared, this was due to the new formed hydroxyl protons after the reaction between epoxy and carboxyl acid groups. In addition, aliphatic proton of lignin was shifted to 1.51 ppm and 1.54 ppm assigned to the aliphatic protons in the side chains of KH560. The successful chemical reaction indicated that the interface interactions between the lignin and PLA were improved after addition of KH560.

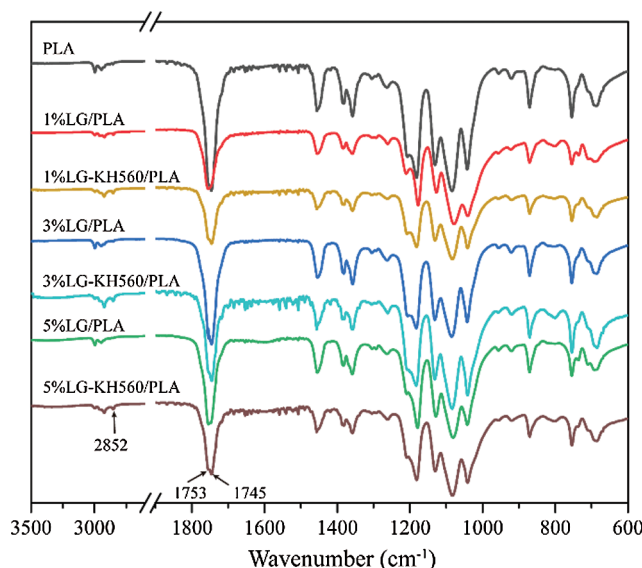


**Figure 2:** The ATR spectra of PLA and its composites

### 3.3 Thermal Properties

Fig. 4a shows the second run DSC heating curves of pure PLA and its composites. Three notable temperatures on graphs can be observed, namely the glass transition, cold crystallization and melting temperatures. Glass transition is a sophisticated effect which relies on the interactions between the molecules, steric effects, flexibility of molecular chains, molecular weight and density of cross-linking of

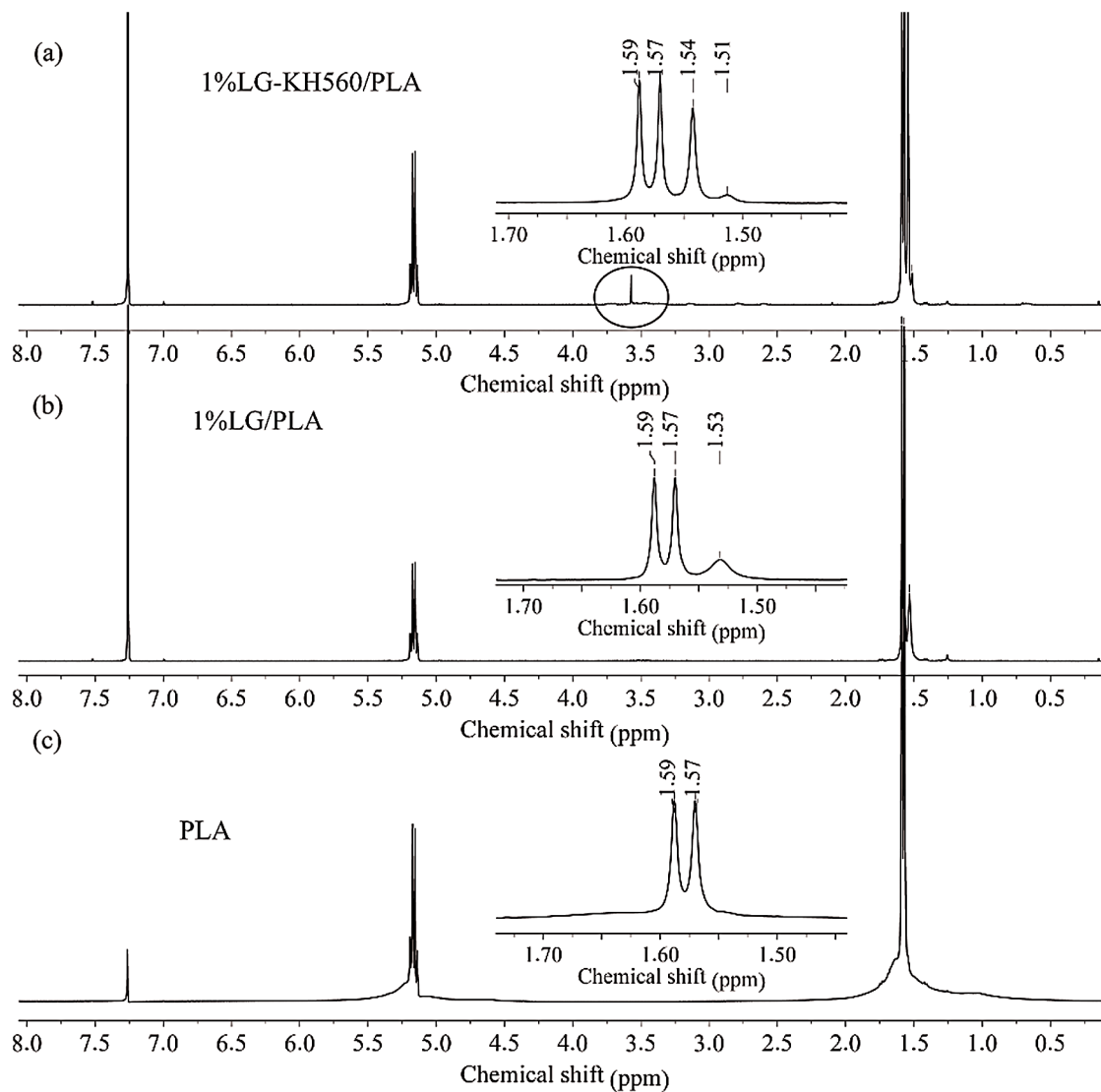


**Figure 3:** The  $^1\text{H}$  NMR spectra of PLA and its composites

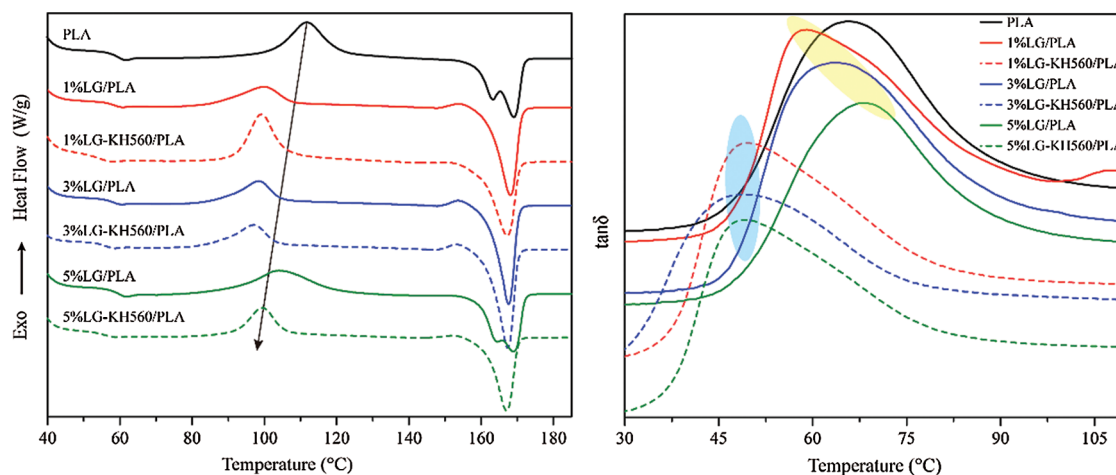


**Figure 4:** (a) DSC and (b) DMA curves of PLA and its composites

a polymer [21,22]. Introduction of a new phase into the polymer matrix may enhance, weaken or make no difference on the glass transition.

As shown in Tab. 2 and Fig. 4, both DSC and DMA results proved that the  $T_g$  of PLA/lignin composites with KH560 were lower than that of unmodified. The decrease in  $T_g$  means that KH560 modified PLA/lignin requires less energy for the movement of molecular chains. This phenomenon is attributed to the fact that the excess silane may cause lubrication effect, and then increase the molecular chain mobility.

**Table 2:** Thermal analysis data for PLA and its composites

	$T_g^a$ (°C)	$T_g^b$ (°C)	$T_{cc}$ (°C)	$\Delta H_{cc}$ (J/g)	$T_m$ (°C)	$\Delta H_m$ (J/g)	$\chi_c$ (%)
PLA	58.98	66.6	112.75	26.78	165.60	29.66	3.09
1%LG/PLA	56.83	59.2	99.43	13.1	168.35	41.7	31.03
3%LG/PLA	57.84	63.6	98.60	19.4	167.68	47.5	31.11
5%LG/PLA	60.39	64.7	104.89	20.6	167.75	47.9	33.38
1%LG-KH560/PLA	54.97	48.2	99.07	26.2	167.15	34.9	9.44
3%LG-KH560/PLA	56.32	50.2	97.41	20.0	167.30	38.6	20.60
5%LG-KH560/PLA	56.20	48.9	99.25	17.4	167.06	34.4	19.22

a. Values obtained from DSC

b. Values obtained from DMA

The cold crystallization temperatures ( $T_{cc}$ ) of pure PLA and its composites obtained from the second run heating curves were shown in Tab. 2.  $T_{cc}$  represents an exothermic peak due to the crystallization of the polymer matrix. The  $T_{cc}$  of the pure PLA was 112.75°C. Cold crystallization is a behavior due to the complex interaction between the crystallization kinetics and potential for crystallization. The introduction of a second phase can influence the kinetics, typically via the restriction of chain mobility that is critical during crystallization. Moreover, a second phase can supply a platform that may promote crystallization by lowering the free energy required for nucleation and ultimately impacting the crystallization's potential [22]. In the case of 1%LG/PLA and 3%LG/PLA, the cold crystallization peak temperature shifted to lower temperature. This effect is due to a rise in surface area for heterogeneous nucleation, which in turn causes an increase in the crystal-forming tendency, thus favoring crystals to form at colder conditions. The low temperature crystal-forming phenomenon was different in the scenario of 5%LG/PLA, where the cold crystallization peak temperature shifts to higher temperature. This phenomenon is due to the fact that the resistance to the movement of the molecular chains required for crystallization increases more than the rise in crystal-forming potential due to heterogeneous nucleation. The addition of KH560 to the PLA/lignin composites gave lower  $T_{cc}$  values than those composites without addition of KH560. After modified by KH560, the cold crystallization temperature of all three components composites shifted to lower temperature. The reason for this maybe that the long liner aliphatic side chain of KH560 can act as heterogeneous nucleating agent resulting in a decrease in crystallization potential. Compared to KH560 modified composites, the unmodified lignin was less suitable to bond with PLA. This results in steric hindrance which restricts the molecular chain motion of PLA. Furthermore, it constrained the crystallization of PLA, result of high  $T_g$  and  $T_{cc}$  values.

Pure PLA showed a double endothermic peak at 165.60°C and 170.77°C. This double peak is commonly in polyesters, and this mainly because the melt/recrystallization/re-melt mechanism [23]. In this work, all composites showed almost similar melting peak temperatures.

The degree of crystallinity ( $\chi_c$ ) of the pure PLA and its composites were calculated by the expression (1):

$$\chi_c = \frac{\Delta H_m - \Delta H_{cc}}{\Delta H_m^0 w} \times 100\% \quad (1)$$

where  $\Delta H_m$  represents the experimental melting enthalpy (J/g),  $\Delta H_0$  denotes the melting enthalpy of 100% crystalline PLA (93.7 J/g) and  $w$  symbolizes the weight fraction of PLA in the composites.

As shown in Tab. 2, the  $\chi_c$  of PLA/lignin composites was decreased after addition of KH560. This is mainly due to (1) the increased compatibility of lignin and PLA and the reduced number of nucleating agents in composite systems with the presence of KH560, and (2) the fact that KH560 connects lignin and PLA by chemical bonding, the molecular chain motility is reduced and the crystallization rate is reduced. It is commonly accepted that the polymers' toughening by filler is followed by a corresponding drop in the, crystallization temperature,  $T_g$ , melting temperature, and decrease in crystallinity [24,25]. Thereafter, with the toughening effect by KH560, the PLA/lignin composites' thermodynamic properties were lessened.

Fig. 5 shows the TGA curves of pure PLA and its composites. Tab. 3 summarized the composites' thermal degradation temperature parameters. The thermal stability of KH560 unmodified composites was comparatively higher than modified composites. This mainly due to the weak compatibility between PLA and lignin that thwarted the exchange of heat within the composites. The enhancement of the interfacial interactions between the two phases was achieved with the employment of coupling agent KH560 and it promoted heat conduction. As lignin amount increased, the interfacial molecular chains of PLA were securely bounded together due to effective interaction of the coupling agent and more energy was required to weaken the chemical and physical interactions. This translated to sound thermal degradation behavior.

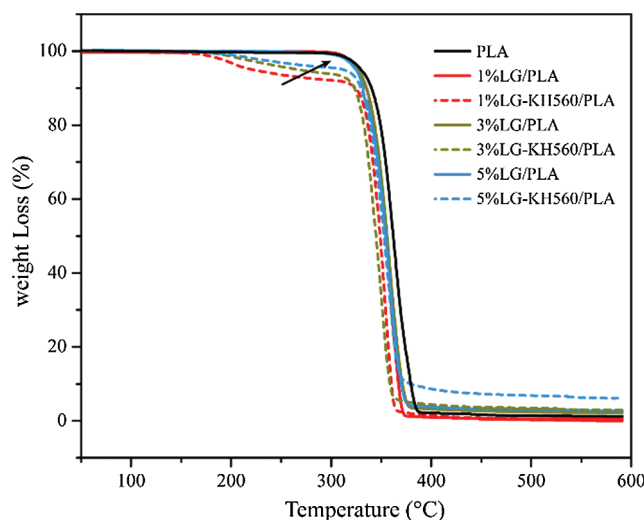


**Figure 5:** Thermal degradation of PLA and its composites

### 3.4 Mechanical Properties

Tab. 4 depicts the mechanical properties of PLA and its composites. The maximum strain of the composites was not severely affected by the addition of lignin and KH560. The decrease in tensile strength of LG/PLA composites can be credited to the poor interfacial adhesion between lignin particles and the PLA matrix. The addition of 5 wt% loading of lignin into PLA caused a considerable drop in tensile strength. This is mainly because the lignin particles aggregated and formed agglomerates in PLA

**Table 3:** Thermogravimetric analysis data of PLA and its composites

	T <sub>5%</sub> (°C)	T <sub>50%</sub> (°C)	T <sub>max</sub> (°C)	Carbon residue rate (%)
Pure PLA	326.57	358.86	588.89	1.22
1%LG/PLA	326.09	354.86	590.89	1.34
3%LG/PLA	322.99	352.01	588.54	2.15
5%LG/PLA	320.64	350.98	587.90	2.73
1%LG-KH560/PLA	185.53	354.76	761.17	1.57
3%LG-KH560/PLA	250.80	351.78	781.94	2.92
5%LG-KH560/PLA	296.73	349.61	786.07	6.06

**Table 4:** Mechanical properties of PLA and its composites

Sample	Tensile strength (MPa)	Young's modulus (MPa)	Elongation at break (%)
Pure PLA	52.5 ± 0.3	3065 ± 15	6.9 ± 0.4
1%LG/PLA	49.5 ± 0.1	3089 ± 10	6.4 ± 0.3
3%LG/PLA	45.7 ± 0.2	3188 ± 3	5.7 ± 0.5
5%LG/PLA	45.7 ± 0.6	3237 ± 19	5.6 ± 0.3
1%LG-KH560/PLA	50.6 ± 0.2	3230 ± 12	6.3 ± 0.2
3%LG-KH560/PLA	49.3 ± 0.3	3287 ± 17	6.0 ± 0.4
5%LG-KH560/PLA	52.4 ± 0.2	3413 ± 16	6.1 ± 0.3

matrix. For KH560 modifications, the coupling agent molecules link the PLA and lignin together, which significantly improved the adhesive force between the interfaces of two components. After modification of the KH560, the tensile strength was increased from 45.7 MPa of 5%LG/PLA to 50 MPa in 5%LG-KH560/PLA; matching that of pure PLA (52.4 MPa) and demonstrated the efficacy of the compatibilizer. The chemical reactions at the interfaces provide the composites with better mechanical properties than PLA filled with untreated lignin.

In this work, the PLA/lignin composites' tensile strength which was synthesized in a single-step manner (in situ formation of the compatibilizer by incorporating PLA, lignin and coupling agent KH560 straight) is relatively lower than that of the composites made by a two-step method (first the lignin is treated by silane coupling agent solution and then added into polymer matrix). Zhu et al. reported using solution treatment method to make PLA/lignin composite, when the lignin loading increased 20 wt%, the KH560 modified composite could still maintain about 53 MPa [19]. The relatively lower tensile strength of the PLA/lignin composite through one-step reactive compatibilization, the existence of free radicals from the coupling agents results in deterioration of the whole composite's polymer matrix and this could lessen the tensile properties [26,27].

#### 4 Conclusions

To clarify the effects of lignin as a biodegradable filler added into the PLA matrix, PLA/lignin composites with or without coupling agent KH560 were prepared by a one-step solvent-free modification method. The effects of KH560 as a compatibilizer on the morphology, chemical structure, crystallization

behavior, thermal degradative behavior as well as mechanical strength of the PLA/lignin composites were analyzed in detail. It was found that, after modification by KH560, the fractured surfaces of composites became smooth, suggested sufficient adhesion between the lignin and PLA in the composites with KH560 coupling agent molecules. This result further proved by  $^1\text{H}$  NMR and ATR spectra of the composites that lignin and PLA formed stable chemical bonds with KH560. Due to the toughening effect of KH560, mainly affect the molecular chain mobility, the thermodynamic properties of LG-KH560/PLA samples were all reduced. When compared to the conventional solution modification method of adding silane coupling agents into PLA/lignin, the composites were synthesized via a single-step solvent-free modification process in this work showed relatively low tensile strength, which mainly because the existence of the free radicals from the coupling agents bring about deterioration in the composite and thus weakening the tensile properties.

**Funding Statement:** This study was funded by the National Key Research and Development Program of China (grant number: 2019YFD1101201), the National Natural Science Foundation of China (grant numbers: 51773005 and 21905008) and the Beijing Natural Science Foundation (grant number: 2194071).

**Conflicts of Interest:** The authors declare that they have no conflicts of interest to report regarding the present study.

## References

1. Oksman, K., Skrifvars, M., Selin, J. F. (2003). Natural fibres as reinforcement in polylactic acid (PLA) composites. *Composites Science and Technology*, 63(9), 1317–1324. DOI 10.1016/S0266-3538(03)00103-9.
2. Chung, Y. L., Olsson, J. V., Li, R. J., Frank, C. W., Waymouth, R. M. et al. (2013). A renewable lignin-lactide copolymer and application in biobased composites. *ACS Sustainable Chemistry & Engineering*, 1(10), 1231–1238. DOI 10.1021/sc4000835.
3. Rasal, R. M., Janorkar, A. V., Hirt, D. E. (2010). Poly (lactic acid) modifications. *Progress in Polymer Science*, 35(3), 338–356. DOI 10.1016/j.progpolymsci.2009.12.003.
4. Nofar, M., Sacligil, D., Carreau, P. J., Kamal, M. R., Heuzey, M. C. (2019). Poly (lactic acid) blends: processing, properties and applications. *International Journal of Biological Macromolecules*, 125, 307–360. DOI 10.1016/j.ijbiomac.2018.12.002.
5. Wen, X., Liu, Z. Q., Li, Z., Zhang, J., Wang, D. Y. et al. (2020). Constructing multifunctional nanofiller with reactive interface in PLA/CB-g-DOPO composites for simultaneously improving flame retardancy, electrical conductivity and mechanical properties. *Composites Science and Technology*, 188, 107988.
6. Popper, Z. A. (2008). Evolution and diversity of green plant cell walls. *Current Opinion in Plant Biology*, 11(3), 286–292. DOI 10.1016/j.pbi.2008.02.012.
7. Mendu, V., Harman-Ware, A. E., Crocker, M., Jae, J., Stork, J. et al. (2011). Identification and thermochemical analysis of high-lignin feedstocks for biofuel and biochemical production. *Biotechnology for Biofuels*, 4(1), 43. DOI 10.1186/1754-6834-4-43.
8. Ten, E., Vermerris, W. (2015). Recent developments in polymers derived from industrial lignin. *Journal of Applied Polymer Science*, 132(24), 21. DOI 10.1002/app.42069.
9. Guo, X., Zhang, S., Shan, X. Q. (2008). Adsorption of metal ions on lignin. *Journal of Hazardous Materials*, 151(1), 134–142. DOI 10.1016/j.jhazmat.2007.05.065.
10. Kun, D., Pukánszky, B. (2017). Polymer/lignin blends: interactions, properties, applications. *European Polymer Journal*, 93, 618–641. DOI 10.1016/j.eurpolymj.2017.04.035.
11. Gordobil, O., Egues, I., Llano-Ponte, R., Labidi, J. (2014). Physicochemical properties of PLA lignin blends. *Polymer Degradation and Stability*, 108, 330–338. DOI 10.1016/j.polymdegradstab.2014.01.002.
12. Dai, L., Liu, R., Si, C. L. (2018). A novel functional lignin-based filler for pyrolysis and feedstock recycling of poly (L-lactide). *Green Chemistry*, 20(8), 1777–1783. DOI 10.1039/C7GC03863A.

13. Zhou, Y. H., Fan, M. Z., Chen, L. H. (2016). Interface and bonding mechanisms of plant fibre composites: an overview. *Composites Part B: Engineering*, 101, 31–45. DOI 10.1016/j.compositesb.2016.06.055.
14. George, J., Sreekala, M. S., Thomas, S. (2001). A review on interface modification and characterization of natural fiber reinforced plastic composites. *Polymer Engineering and Science*, 41(9), 1471–1485. DOI 10.1002/pen.10846.
15. Anwer, M. A. S., Naguib, H. E., Celzard, A., Fierro, V. (2015). Comparison of the thermal, dynamic mechanical and morphological properties of PLA-Lignin & PLA-Tannin particulate green composites. *Composites Part B: Engineering*, 82, 92–99. DOI 10.1016/j.compositesb.2015.08.028.
16. Chen, L., Tang, C. Y., Ning, N. Y., Wang, C. Y., Fu, Q. et al. (2009). Preparation and properties of chitosan/lignin composite films. *Chinese Journal of Polymer Science*, 27(5), 739–746. DOI 10.1142/S0256767909004448.
17. Qian, S. P., Sheng, K. C. (2017). PLA toughened by bamboo cellulose nanowhiskers: role of silane compatibilization on the PLA bionanocomposite properties. *Composites Science and Technology*, 148, 59–69. DOI 10.1016/j.compscitech.2017.05.020.
18. Tang, Y. S., Dong, W. C., Tang, L., Zhang, Y. K., Kong, J. et al. (2018). Fabrication and investigations on the polydopamine/KH-560 functionalized PBO fibers/cyanate ester wave-transparent composites. *Composites Communications*, 8, 36–41. DOI 10.1016/j.coco.2018.03.006.
19. Lv, H., Song, S., Sun, S., Ren, L., Zhang, H. (2016). Enhanced properties of poly (lactic acid) with silica nanoparticles. *Polymers for Advanced Technologies*, 27(9), 1156–1163. DOI 10.1002/pat.3777.
20. Zhu, J., Xue, L. Y., Wei, W., Mu, C. Y., Jiang, M. et al. (2015). Modification of lignin with silane coupling agent to improve the interface of Poly (L-lactic) acid/lignin composites. *BioResources*, 10(3), 4315–4325. DOI 10.15376/biores.10.3.4315-4325.
21. Krishnamachari, P., Zhang, J., Lou, J. Z., Yan, J. Z., Uitenham, L. (2009). Biodegradable poly (lactic acid)/clay nanocomposites by melt intercalation: a study of morphological, thermal, and mechanical properties. *International Journal of Polymer Analysis and Characterization*, 14(4), 336–350. DOI 10.1080/10236660902871843.
22. Frone, A. N., Berlioz, S., Chailan, J. F., Panaitescu, D. M. (2013). Morphology and thermal properties of PLA-cellulose nanofibers composites. *Carbohydrate Polymers*, 91(1), 377–384. DOI 10.1016/j.carbpol.2012.08.054.
23. Ma, P. M., Wang, R. Y., Wang, S. F., Zhang, Y., Zhang, Y. X. et al. (2008). Effects of fumed silica on the crystallization behavior and thermal properties of poly (hydroxybutyrate-co-hydroxyvalerate). *Journal of Applied Polymer Science*, 108(3), 1770–1777. DOI 10.1002/app.27577.
24. Saeidlou, S., Huneault, M. A., Li, H. B., Park, C. B. (2012). Poly (lactic acid) crystallization. *Progress in Polymer Science*, 37(12), 1657–1677. DOI 10.1016/j.progpolymsci.2012.07.005.
25. Liu, H., Zhang, J. (2011). Research progress in toughening modification of poly (lactic acid). *Journal of Polymer Science Part B: Polymer Physics*, 49(15), 1051–1083. DOI 10.1002/polb.22283.
26. Nyambo, C., Mohanty, A. K., Misra, M. (2011). Effect of maleated compatibilizer on performance of PLA/wheat straw-based green composites. *Macromolecular Materials and Engineering*, 296(8), 710–718. DOI 10.1002/mame.201000403.
27. Zhang, J. F., Sun, X. Z. (2004). Mechanical properties of poly (lactic acid)/starch composites compatibilized by maleic anhydride. *Biomacromolecules*, 5(4), 1446–1451. DOI 10.1021/bm0400022.